https://ntrs.nasa.gov/search.jsp?R=19980227310 2020-06-15T23:06:55+00:00Z

NASA TN D-482

TECHNICAL NOTE

D-482

AN ANALYSIS OF NUCLEAR-ROCKET NOZZLE COOLING

By William H. Robbins, Daniel Bachkin,
and Arthur A. Medeiros

Lewis Research Center
Cleveland, Ohio

NATIONAL AERONAUTICS AND SPACE ADMINISTRATION
WASHINGTON
November 1960

NATIONAL AERONAUTICS AND SPACE ADMINISTRATION

TECHNICAL NOTE D-482

AN ANALYSIS OF NUCLEAR-ROCKET NOZZLE COOLING

By William H. Robbins, Daniel Bachkin,
and Arthur A. Medeiros

E-824

CQ-1

SUMMARY

A nuclear-rocket regenerative-cooling analysis was conducted over a range of reactor power of 46 to 1600 megawatts and is summarized herein. Although the propellant (hydrogen) is characterized by a large heat-sink capacity, an analysis of the local heat-flux capability of the coolant at the nozzle throat indicated that, for conventional values of system pressure drop, the cooling capability was inadequate to maintain a selected wall temperature of 1440° R. Several techniques for improving the cooling capability were discussed, for example, high pressure drop, high wall temperature, refractory wall coatings, thin highly conductive walls, and film cooling. In any specific design a combination of methods will probably be utilized to achieve successful cooling.

INTRODUCTION

Gas-cycle nuclear-rocket powerplants with hydrogen as a propellant are being seriously considered as propulsion devices for space vehicles because of the high specific impulse associated with these systems. For example, a specific impulse of 900 pounds per pound per second can be obtained at a chamber gas temperature of approximately 4700° R.

Mission studies have been conducted to establish the powerplant requirements for nuclear-rocket systems. These analyses are concerned with two general types of missions: (1) takeoff from the earth, and (2) takeoff from orbit. Both were considered in the investigation of reference 1. The majority of the discussion of reference 1 is devoted to orbital takeoff, since it appears to be more practical at the present time, primarily because the powerplant requirements and site-contamination problems are less severe.

Nuclear-rocket component development is also proceeding rapidly. For example, the Los Alamos Scientific Laboratory has constructed a reactor for nuclear-rocket application (ref. 2). In addition, hydrogen turbopump studies have been made, and the results of one typical study are reported in reference 3.

Although many detailed nozzle-cooling studies have been conducted for chemical rockets (e.g., ref. 4), little consideration has thus far been given to nuclear-rocket nozzle cooling, primarily because no problem has been anticipated, particularly when hydrogen, which has a large heat-sink capacity, is used as the propellant. A more complete analysis of nozzle cooling appears warranted and is presented in this paper. This report can be categorized as a preliminary design study of nuclear-rocket nozzle cooling. The range of variables, therefore, does not necessarily cover the complete nuclear-rocket design spectrum; however, the scope was sufficient to manifest the critical problem areas. The material presented covers a range of reactor power of 46 to 1600 megawatts and includes the heat transfer to the nozzle wall and to the coolant. The variation of the cooling capability over a range of pressure and wall temperature is also indicated. In addition, other techniques for improving the cooling capability, such as refractory wall coatings and film cooling, are discussed. This investigation was conducted at the NASA Lewis Research Center.

E-824

SYMBOLS

b	wall thickness
c_p	specific heat at constant pressure
d	diameter
h	heat-transfer coefficient
h_g	heat-transfer coefficient based on enthalpy
i	enthalpy
i_{ref}	reference enthalpy
k	thermal conductivity
Nu	Nusselt number, hd/k
Pr	Prandtl number, $\mu c_p/k$
p	pressure
q	heat flux
R	gas constant
Re	Reynolds number, $\rho Vd/\mu$

t	temperature
V	velocity
z	compressibility factor
μ	absolute viscosity
ρ	density

Subscripts:

ad	adiabatic wall
B	coolant
f	film conditions
g	gas side
H	hydraulic
i,ref	reference enthalpy
s	stream
t	total
w	wall
0	stagnation conditions

E-824
CQ-1 back

POWERPLANT DESCRIPTION AND OPERATING CONDITIONS

A schematic diagram of a typical nuclear-rocket system is shown in figure 1. The powerplant includes a propellant tank, a turbopump, a reactor, and a nozzle. For low-pressure systems a pressurized tank system may be used instead of a turbopump. In either case, the propellant is forced through the nozzle cooling jacket and the reflector in order to cool these components. The propellant then passes through the reactor core, where it is heated to the highest temperature possible consistent with the reactor materials. The hot propellant is then expanded to supersonic velocities through a nozzle and thus produces propulsive thrust.

The reactor and nozzle geometries used in the nozzle heat-transfer analysis reported herein are those resulting from a mission study, conducted at the NASA, similar to that reported in reference 1. Hydrogen was used as the propellant. The reactor core diameter was determined, primarily from nuclear criticality considerations, to be 24 inches. This value, which is also the nozzle-inlet diameter, was held constant over the range of power used in the nozzle heat-transfer analysis. The propellant temperature at the reactor exit was assumed to be limited by reactor structural considerations to 4680° R (2600° K). This value, which is referred to as the nozzle chamber temperature, was held constant throughout the analysis. The reactor power was varied by variations in the propellant flow rate. The propellant flow rate can be varied by changes in the nozzle throat diameter or the nozzle chamber pressure. For convenience in the analysis, the nozzle throat diameter was held fixed, and the investigation was conducted over a range of chamber pressures. The nozzle throat diameter was 6 inches, and the exit- to throat-area ratio was assumed as 50. The nozzle was 58 inches long. A range of chamber pressure of 44.1 to 1470 pounds per square inch absolute was investigated.

The range of dependent propulsion-system variables, pertinent to the nozzle, was calculated from the assumptions just given and the properties of hydrogen under chemical equilibrium conditions given in reference 5. There is some evidence (ref. 6) that frozen composition rather than equilibrium composition should have been assumed in the calculation procedure. However, the differences between frozen and equilibrium conditions over the range of temperature and pressure considered in this analysis are negligible. The calculated variables, propellant flow, reactor power, engine thrust, and vacuum specific impulse, are shown in figure 2. As chamber pressure is increased from 44.1 to 1470 pounds per square inch absolute, propellant flow increases from 2.4 to 83 pounds per second, reactor power increases from 46 to 1600 megawatts, and engine thrust increases from 2200 to 73,000 pounds. In contrast, the vacuum specific impulse decreases slightly, from 900 to 880 seconds (about 2 percent). This is due to the decreased amount of dissociated products as pressure is increased.

GAS-SIDE HEAT TRANSFER

Three modes of heat transfer to the nozzle wall were considered: (1) the convective heat transfer from the propellant, (2) the thermal radiation from the reactor face, and (3) gamma heating of the nozzle wall.

Convective Heat Transfer

The convective heat transfer from the propellant to the nozzle walls was evaluated for a fixed wall temperature assuming fully developed turbulent pipe flow. As recommended in reference 7, the heat transfer was computed on an enthalpy basis from the following equation:

$$Nu = 0.023(Re)^{0.8}(Pr)^{1/3} \tag{1}$$

By algebraic manipulation of equation (1) the expression for the heat-transfer coefficient becomes:

$$h_g = \frac{h}{c_p} = \frac{0.023}{d^{0.2}} (\rho_s V_s)^{0.8} \left(\frac{t_s}{t_{i,ref}}\right)^{0.8} \frac{(\mu)^{0.2}_{i,ref}}{(Pr)^{2/3}_{i,ref}} \tag{2}$$

As recommended in reference 7 (pp. 261-272), the transport properties (c_p, μ, and k) and density ρ were evaluated at reference enthalpy. The reference enthalpy (ref. 7) is given as

$$i_{ref} = i_f + 0.22(Pr)^{1/3}_{i,ref}(i_0 - i_s) \tag{3}$$

The convective heat flux q_g was then obtained from the following equation:

$$q_g = h_g(i_{ad} - i_w) \tag{4}$$

where

$$i_{ad} = i_s + (Pr)^{1/3}_{i,ref}(i_0 - i_s) \tag{5}$$

The variation of convective heat flux with nozzle length for various chamber pressures is presented in figure 3 for a chamber temperature of 4680° R and a wall temperature of 1440° R. Although the wall temperature is somewhat below the value that can be maintained with conventional materials such as nickel and stainless steel, it is commensurate with chemical-rocket practice and provides a margin of safety should local "hot spots" occur on the nozzle wall. A schematic diagram of the nozzle is also shown. As expected, the convective-heat-transfer rate increases rapidly along the convergent section of the nozzle. The heat flux reaches a maximum value at the nozzle throat and decreases rapidly through the divergent section. Maximum values of heat flux (at the throat) range from 3.1 Btu/(sec)(sq in.) at a chamber pressure of 44.1 pounds per square inch absolute to 51 Btu/(sec)(sq in.) at the highest chamber pressure investigated (1470 lb/sq in. abs).

Radiation Heat Transfer

The heat flux as a result of thermal radiation from the reactor face to the nozzle wall is shown in figure 4 for an estimated face temperature of 4680° R and a wall temperature of 1440° R. It was assumed that the reactor face and nozzle walls were black (emissivity, 1). The calculation procedure is outlined in reference 7 (pp. 395-418). Since the propellant gas is transparent, the radiant heat flux is independent of chamber pressure. As indicated in figure 4(a), values of radiant heat flux rise very rapidly from the nozzle inlet to a maximum value of 1.08 Btu/(sec)(sq in.) at approximately 6 percent of the nozzle length. The radiant heat-transfer rate then decreases to values approaching zero just beyond the nozzle throat. The ratio of radiant heat flux to total heat flux is also shown (fig. 4(b)) for various chamber pressures. At low values of chamber pressure, the radiant heat flux represents a very significant part of the total heat flux in the convergent section of the nozzle. The effect of thermal radiation diminishes as chamber pressure is increased; however, even at the highest chamber pressure (1470 lb/sq in. abs) the radiant heat flux represents 13 to 18 percent of the total heat flux near the reactor face (2 to 10 percent of the nozzle length).

Nuclear Heating

The contribution of the gamma heating along the nozzle wall was determined from conventional calculation techniques presented in reference 8. The variation of gamma heating in the nozzle walls with nozzle length over a range of chamber pressures is shown in figure 5. It was assumed that the nozzle was fabricated from nickel and had a 0.020-inch-thick wall. The maximum value of heat flux, 0.37 Btu/(sec)(sq in.), occurred at the nozzle inlet at a chamber pressure of 1470 pounds per square inch absolute (fig. 5(a)). At a fixed value of chamber pressure (reactor power), the gamma heating decreased approximately linearly along the nozzle length, and, as expected, the magnitude of the gamma heating also decreased with reactor power. The gamma heating in terms of the total heat flux (fig. 5(b)) was less than 8 percent at all nozzle axial positions.

Total Heat-Flux Rate

To summarize the gas-side local heat-transfer rate, curves of the total heat flux were plotted against nozzle length (fig. 6) for the chamber and wall conditions previously described. The total heat flux is a summation of the convective, thermal radiation, and gamma heat fluxes presented in figures 3 to 5. Maximum values of total heat flux (at the

throat) range from 3.2 Btu/(sec)(sq in.) at a chamber pressure of 44.1 pounds per square inch absolute to 51.8 Btu/(sec)(sq in.) at a chamber pressure of 1470 pounds per square inch absolute. From a comparison of figures 6 and 3 it is apparent that the thermal radiation and nuclear heat generation are appreciable percentages of the total heat flux in the convergent portion of the nozzle. In contrast, at the throat, where the maximum heat flux occurs, and in the divergent section of the nozzle the heat flux is essentially unchanged by thermal radiation or nuclear heat generation.

E-874

HEAT TRANSFER TO COOLANT

In analyzing the capabilities of the coolant, two conditions must be considered: (1) the heat-sink capacity of the coolant as compared with the total heat flow it is required to absorb, and (2) the capability of the coolant to absorb heat at the required rate for the desired wall temperature.

Coolant Heat-Sink Capacity

The integration of the local values of total heat flux (fig. 6) over the nozzle area represents the total heat flow that must be absorbed by the coolant if satisfactory cooling is to be achieved. The total heat flow and coolant temperature rise across the nozzle are plotted against chamber pressure for constant chamber and wall temperatures of 4680° and 1440° R, respectively, in figure 7. As expected, the total heat flow increases with chamber pressure because the local heat flux along the nozzle rises with increased chamber pressure (fig. 6). In contrast, the coolant temperature rise decreases with increasing chamber pressure. Values of coolant temperature rise range from approximately 200° R at the lowest chamber pressure investigated (44.1 lb/sq in. abs) to 75° R at the highest chamber pressure (1470 lb/sq in. abs). The decrease in coolant temperature rise with increasing pressure is explained by the fact that coolant flow is increasing linearly with increased pressure, whereas the convective heat flux to the walls, which accounts for most of the heat transfer, is increasing approximately with pressure raised to the 0.8 power. Therefore, the coolant temperature rise varies approximately inversely with pressure raised to the 0.2 power. In view of the relatively low values of coolant temperature rise (200° R max.) over the range of chamber pressure investigated, the coolant (hydrogen) has adequate heat-sink capacity to absorb the relatively high gas-side heat flows.

Local Heat-Flux Capability

In addition to the total heat-sink capacity of the propellant, the local heat-flux capability of the coolant was investigated at three nozzle

axial positions: the inlet, the throat, and the exit. Since the values of heat flux at the nozzle throat were considerably higher than those at the other axial positions (fig. 6), the most severe cooling condition occurs at the throat; for this reason, the major part of the following discussion is concerned with throat conditions.

The coolant convective-heat-transfer coefficient was evaluated from the following equation:

$$h_B = \frac{0.023}{d_H^{0.2}} \frac{c_p(\mu_f)^{0.2}}{(Pr_f)^{2/3}} (\rho_s V_s)^{0.8} \left(\frac{t_s}{t_f}\right)^{0.8} \tag{6}$$

The film temperature was calculated as the average of the fluid bulk temperature and the coolant wall temperature. The coolant wall temperature was determined from the gas-side heat flux, the gas-side wall temperature, the thermal conductivity of the structural wall, and the wall thickness from the following equation:

$$t_{w,B} = t_{w,g} - \frac{b}{k} q_g \tag{7}$$

In all cases analyzed the structural wall was assumed to be nickel, 0.020 inch thick. This again is commensurate with chemical-rocket design procedure. Both the density and transport properties were evaluated at film temperature. Although this technique for computing heat-transfer coefficient differs from the method outlined in reference 4, it was justified on the basis of experimental correlations of heat-transfer data on air and helium at room temperature and higher (refs. 9 and 10).

The heat flux was then calculated as follows:

$$q_B = h_B(t_w - t_{ad}) \tag{8}$$

The total (stagnation) density in the coolant passage was calculated from assigned values of total temperature, total pressure, and the equation of state modified for real-gas effects as follows:

$$\rho_0 = \frac{p_0}{zRt_0} \tag{9}$$

The compressibility factor z for hydrogen was obtained from reference 11. Stream (static) conditions were then obtained from an assigned value of Mach number by means of perfect-gas relations. A temperature- and pressure-dependent value of the isentropic exponent was used.

E-824

A typical variation of coolant heat flux with coolant Mach number is shown in figure 8, where the ratio of coolant heat flux at a given Mach number to the coolant heat flux at a Mach number of 0.7 is plotted against coolant Mach number. The local heat flux that can be absorbed by the coolant increases with increasing coolant Mach number, but reaches a maximum value at a Mach number between 0.7 and 0.8. A coolant Mach number of 0.7 was chosen for the next phase of this analysis. From a heat-transfer standpoint high coolant Mach numbers are most desirable; however, cooling-jacket problems associated with high momentum and friction pressure drops, as well as the practical problem of accurately fabricating coolant passages to avoid flow choking and nozzle burnout, are introduced.

COOLING MARGIN

If a coolant Mach number and wall temperature are assumed, it is possible to compare the rate at which heat is transferred to the wall with the rate at which heat is absorbed by the coolant. The introduction of a new parameter, referred to as the cooling margin, provides a convenient way of making this comparison. The cooling margin was defined as the difference between the coolant and gas-side heat flux divided by the gas-side heat flux $\left(\frac{q_B - q_g}{q_g}\right)$. Positive values of the cooling margin ($q_B > q_g$) indicate satisfactory cooling can be achieved; conversely, negative values indicate insufficient cooling. It should be noted that this parameter is useful for analysis purposes only. In actual nozzle designs, steady-state operating conditions imply that the coolant and gas-side heat flux are equal and the cooling-margin parameter will be zero.

With an assumed Mach number of 0.7 and a wall temperature of 1440° R, the cooling margin at the nozzle throat is plotted in figure 9 against chamber pressure for a range of system pressure ratios of 1.2 to 2.5. The system pressure ratio is the ratio of coolant pressure to chamber pressure and therefore includes both the nozzle coolant pressure drop and the pressure drop across the reactor. Obviously, for a given chamber pressure this parameter fixes the coolant pressure. It should be kept in mind that values of system pressure ratio approaching unity are desirable. Increased system pressure drop at a given chamber pressure means more pump work must be done and therefore more turbine work. If the added work must be done at the expense of bleeding more hydrogen from the nozzle, impulse losses in addition to increases in turbopump weight must be incurred. The maximum value of system pressure drop that can be tolerated, of course, depends on the particular powerplant mission.

It is immediately apparent that, at a wall temperature of 1440° R, the cooling margin at the nozzle throat was inadequate at all values of chamber pressure and system pressure ratio. At a fixed value of chamber pressure, the deficit in cooling margin becomes less as system pressure drop increases, because the coolant heat flux rises with pressure level, whereas the gas side is not affected. At a fixed value of system pressure ratio, the deficit in cooling margin becomes greater with increasing chamber pressure. As chamber pressure increases, both coolant and gas-side heat flux increase, and the temperature drop across the structural wall also increases (eq. (7)). Since the gas-side wall temperature was assumed constant, increased temperature drop across the wall results in a decreased coolant-side wall temperature. Therefore, the gas-side heat flux increases faster than the coolant-side heat flux, and thus the cooling margin is reduced with increasing pressure. It should be noted that thin structural materials with high thermal conductivities will improve the cooling margin, particularly at high values of chamber pressure.

It should be pointed out that increased wall temperature will improve the cooling margin. As indicated previously, somewhat higher values of wall temperature could have been chosen for the analysis. The discussion of the effect of variations in wall temperature on nozzle cooling is presented in detail in the next section.

The local heat-flux capability for the hydrogen nozzle was also investigated at the nozzle entrance and exit stations. It was found that the walls at these axial positions could be cooled to 1440° R with reasonable Mach numbers (less than 0.4) and passage heights over the entire range of variables considered.

Wall Temperature Effects

Inasmuch as the wall temperature is an independent design variable and the value chosen for the preceeding analysis may have been somewhat pessimistic, the cooling margin at the throat was investigated over a range of wall temperature and coolant Mach number. The results of this investigation in curve form are presented in figure 10, where the throat equilibrium wall temperature is plotted against coolant Mach number for a range of system pressure ratio at a chamber pressure of 441 pounds per square inch absolute. The equilibrium wall temperature is the temperature required for a cooling margin of zero. At a coolant Mach number of 0.7 (the value utilized for the previous analysis) the level of equilibrium wall temperature ranges from approximately 1620° R at the highest system pressure ratio (2.5) to 2530° R at the lowest pressure ratio (1.2). As expected, the equilibrium wall temperature increases with decreased coolant Mach number. The equilibrium wall temperatures would be higher at higher chamber pressures and lower at lower chamber pressures; however, the results of figure 10 can be taken as typical. Conventional

fabrication techniques for chemical rockets of brazed tubes or channels of nickel or stainless steel will probably be limited to material temperatures in the range 1500° to 2000° R. For this limiting temperature range, high Mach numbers and large pressure drops will be required for satisfactory cooling. It should be noted that lower Mach numbers are desirable from the viewpoint of pressure drop and flow choking. Thus, as Mach number or pressure drop is reduced, the equilibrium wall temperature increases. These higher wall temperatures will necessitate the use of high-temperature materials and of welded-type construction. These, in turn, may require appreciable development to obtain structurally reliable nozzles.

E-824

Other Techniques for Improving Cooling Margin

In addition to the methods for improving the cooling margin previously presented (by means of pressure and wall temperature variations), there are other techniques available. Two possibilities are suggested: (1) refractory coatings, and (2) film cooling.

CQ-2 back

Refractory materials are characterized by high melting temperatures and low thermal conductivities. Therefore, it may be feasible to protect the structural material of the nozzle with relatively thin refractory coatings. The higher gas-side temperatures possible with coatings will decrease the heat flux to the wall. The low thermal conductivity of the coating will provide a large temperature drop through the coating and thereby maintain low structural metal temperatures. Calculations over the range of conditions considered in the present analysis indicate that coatings of zirconium oxide from 0.005 to 0.015 inch thick achieve successful cooling of the structural nozzle material without exceeding the normal operating temperature of the oxide. Unfortunately, the use of refractory coatings is associated with the practical problems of securely bonding the coating to the metal wall. It should also be pointed out that the temperature gradient in the coating is extremely high (approx. 10^6 deg/in.). This gradient will introduce severe thermal stress in the coating.

Another method that has been considered is film cooling where a fraction of the low-temperature propellant flows along the nozzle walls in order to maintain a specified wall temperature. Unfortunately, film cooling will decrease the specific impulse. The impulse loss due to film cooling, however, may not be as serious as in chemical rockets because nuclear-rocket regenerative cooling is also associated with an impulse loss. This can be explained by the fact that the operating gas temperature of the nuclear rocket is fixed by reactor materials and cannot be increased to compensate for the heat given up to the coolant. At low power levels the regenerative-cooling loss was approximately 2 to 3 percent. The percentage loss, however, decreases with increasing power.

CONCLUDING REMARKS

A nuclear-rocket nozzle regenerative-cooling analysis was conducted over a range of reactor power levels from 46 to 1600 megawatts with hydrogen as a propellant. The following results were obtained in this investigation:

1. The total heat flux to the nozzle walls, which was a summation of the convection from the hydrogen gas, thermal radiation from the reactor face, and nuclear heating, was found to be a maximum at the nozzle throat. For specified chamber and wall temperatures of 4680° and 1440° R, respectively, values of heat flux at the throat ranged from 3.2 to 51.8 Btu/(sec)(sq in.) over a range of chamber pressures of 44.1 to 1470 pounds per square inch absolute.

2. Convection was the dominant mode of heat transfer, particularly at the nozzle throat and in the divergent section. The thermal-radiation heat flux represented a large percentage (60 to 80 percent) of the total heat flux in the convergent section of the nozzle at low values of chamber pressure. The contribution decreased as chamber pressure increased. At high values of chamber pressure (1470 lb/sq in. abs) the gamma heating amounted to about 8 percent of the total heat flux at the nozzle entrance. The gamma heating decreased rapidly to very low levels as chamber pressure was decreased.

3. The hydrogen flowing through the cooling passages had ample total heat-sink capacity, as evidenced by the relatively low temperature rise (200° R max.) across the cooling jacket.

4. An analysis of the local heat-flux capability of the coolant at the nozzle throat (where the gas-side heat flux was a maximum) indicated that the cooling margin was not adequate at a wall temperature of 1440° R, particularly at very high values of chamber pressure.

5. The cooling margin was improved by increased limiting wall temperature. In many cases, this approach alleviates the heat-transfer difficulties, but unfortunately introduces practical nozzle fabricating problems. The cooling margin was also improved by incurring high system pressure losses; however, high pressure drops are usually associated with large impulse losses.

6. In addition to large pressure losses and increased wall temperature, there are several other methods that can be used to improve cooling margin, for example, thin highly conductive nozzle walls, refractory wall

E-824

coatings, high-temperature wall materials, and film cooling. In any specific design a combination of techniques will probably be utilized to achieve a satisfactorily cooled nozzle.

Lewis Research Center
National Aeronautics and Space Administration
Cleveland, Ohio, August 10, 1960

E-824

REFERENCES

1. Rom, Frank E., and Johnson, Paul G.: Nuclear Rockets for Interplanetary Propulsion. Preprint 63R, SAE, 1959.

2. Schreiber, Raemer E.: Los Alamos' Project Rover. Nucleonics, vol. 16, no. 7, July 1958, pp. 70-72.

3. Ginsburg, A. A., Stewart, W. L., and Hartmann, M. J.: Turbopumps for High-Energy Propellants. Rep. 59-53, Inst. Aero. Sci., Inc., 1959.

4. Curren, Arthur N., Price, Harold G., Jr., and Douglass, Howard W.: Analysis of Effects of Rocket-Engine Design Parameters on Regenerative-Cooling Capabilities of Several Propellants. NASA TN D-66, 1959.

5. King, Charles R.: Compilation of Thermodynamic Properties, Transport Properties, and Theoretical Rocket Performance of Gaseous Hydrogen. NASA TN D-275, 1960.

6. Hall, J. Gordon, Eschenroeder, A. Q., and Klein, J. J.: Chemical Nonequilibrium Effects on Hydrogen Rocket Impulse at Low Pressures. Jour. Am. Rocket Soc., vol. 30, no. 2, Feb. 1960, pp. 188-189.

7. Eckert, E. R. G.: Heat and Mass Transfer. McGraw-Hill Book Co., Inc., 1959.

8. Rockwell, Theodore, III, ed.: Reactor Shielding Design Manual. TID 7004, AEC, Mar. 1956.

9. Humble, Leroy V., Lowdermilk, Warren H., and Desmon, Leland G.: Measurements of Average Heat-Transfer and Friction Coefficients for Subsonic Flow of Air in Smooth Tubes at High Surface and Fluid Temperatures. NACA Rep. 1020, 1951. (Supersedes NACA RM's E7L31, E8L03, E50E23, and E50H23.)

10. Taylor, Maynard F., and Kirchgessner, Thomas A.: Measurements of Heat Transfer and Friction Coefficients for Helium Flowing in a Tube at Surface Temperatures up to 5900° R. NASA TN D-133, 1959.

11. Woolley, Harold W., Scott, Russell B., and Brickwedde, F. G.: Compilation of Thermal Properties of Hydrogen in Its Various Isotopic and Ortho-Para Modifications. Jour. Res. Nat. Bur. Standards, vol. 41, no. 5, Nov. 1948, pp. 379-475.

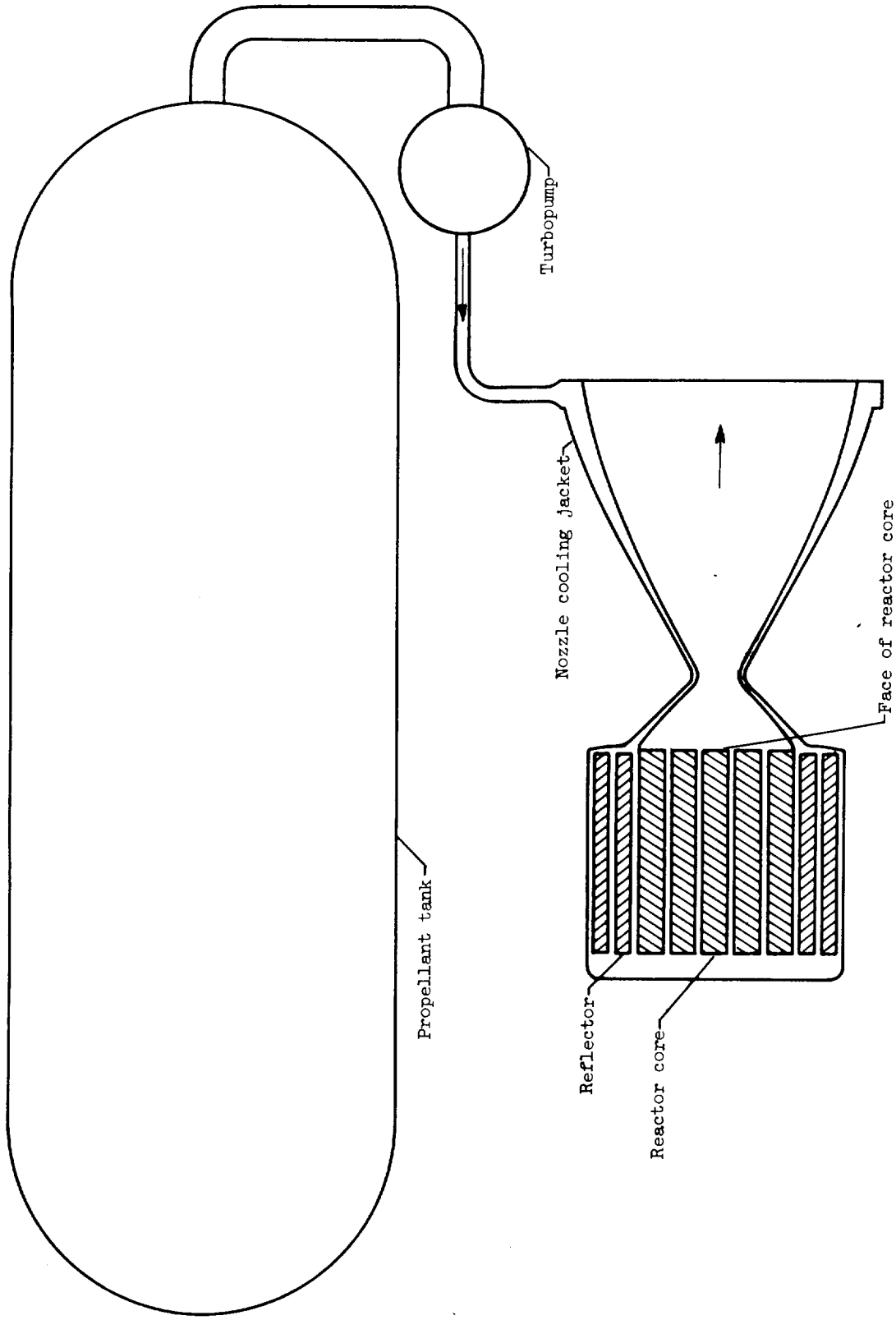

Figure 1. - Schematic diagram of nuclear rocket.

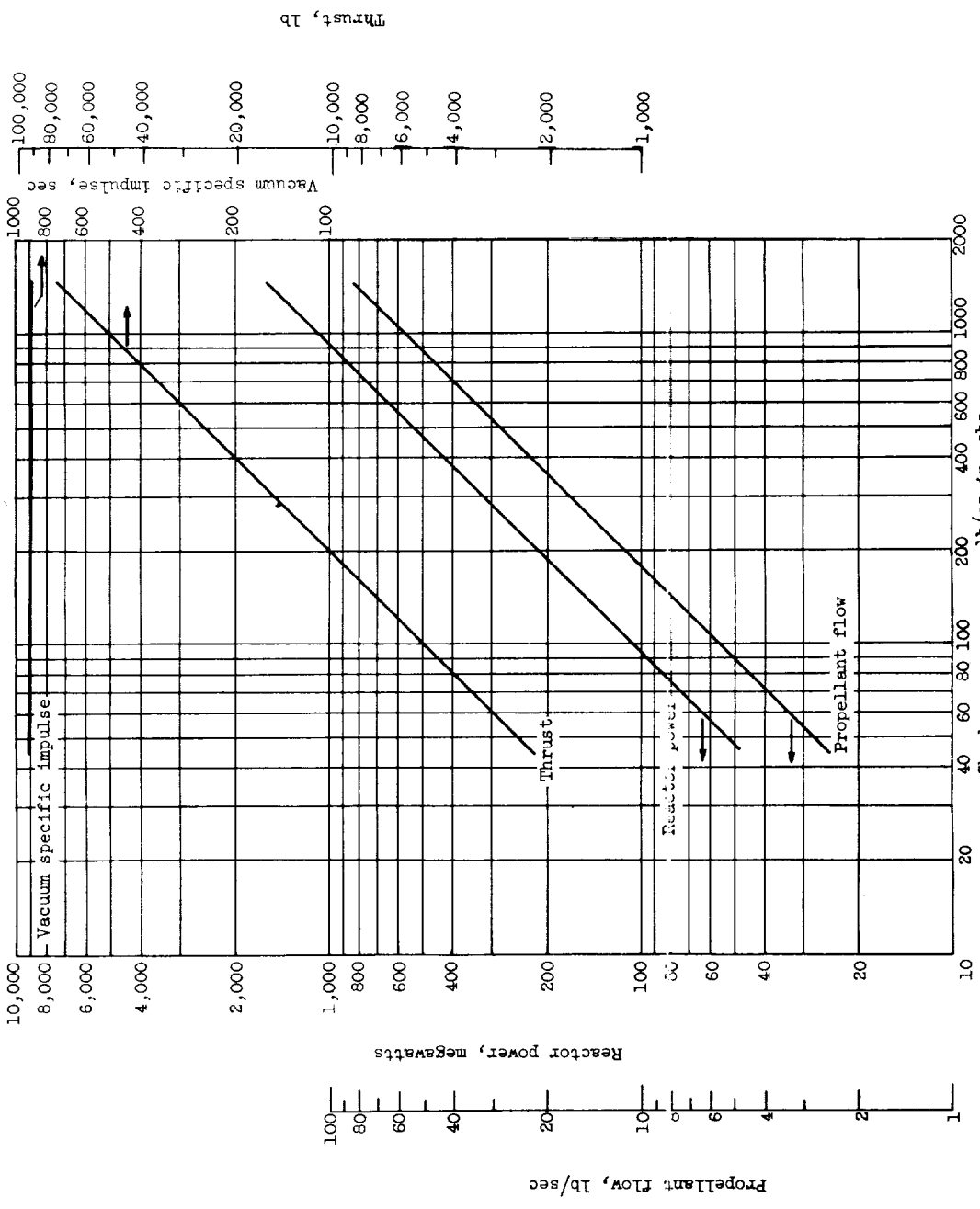

Figure 2. - Powerplant operating conditions.

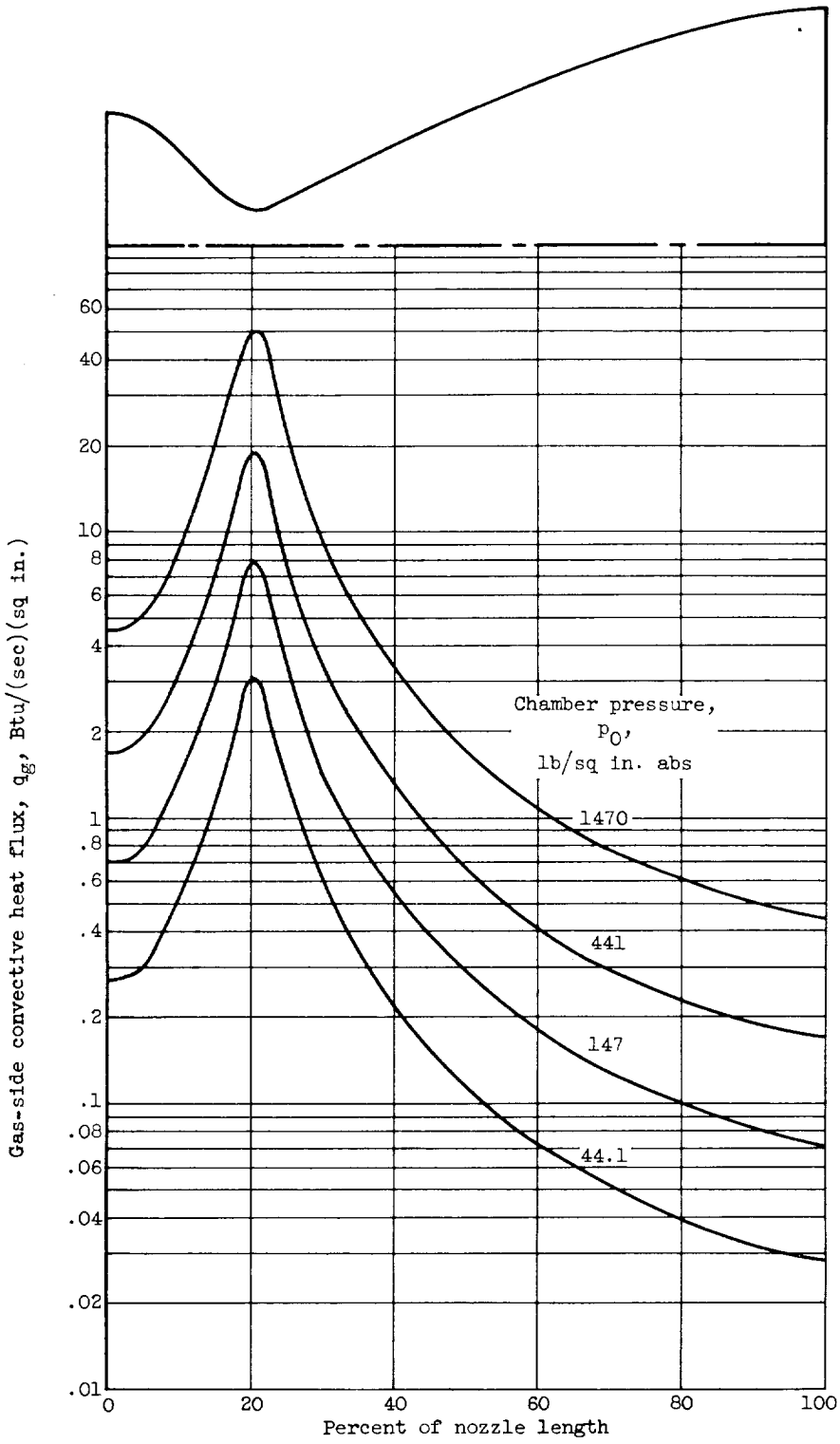

Figure 3. - Variation of convective heat flux with nozzle length for various chamber pressures. Chamber temperature t_o, 4680° R; wall temperature t_w, 1440° R.

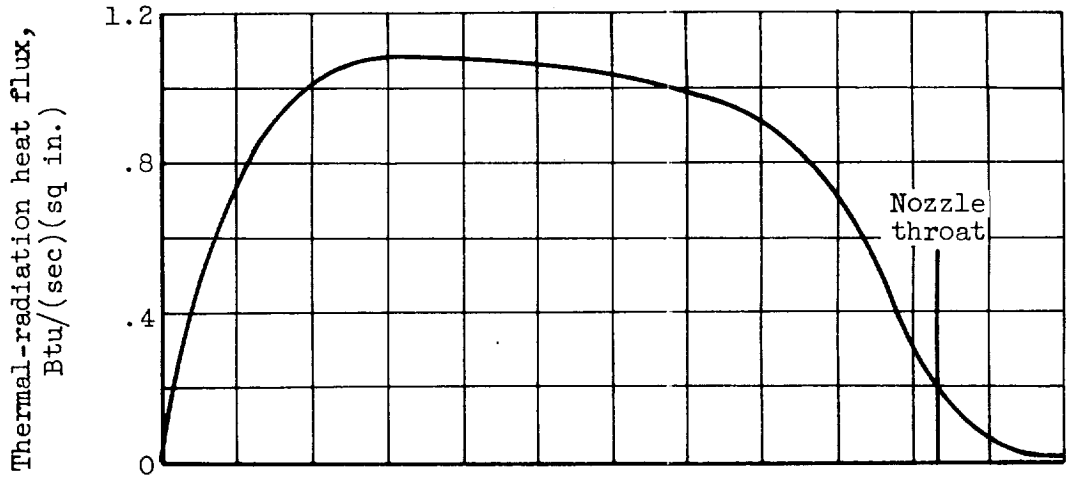

(a) Heat flux.

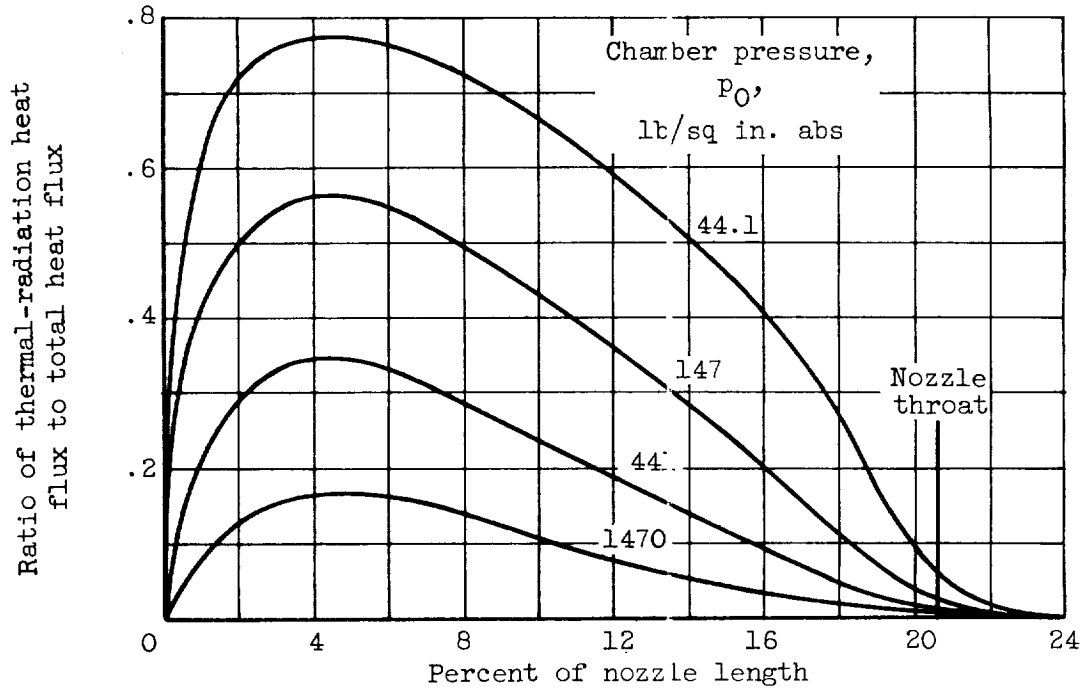

(b) Heat-flux ratio.

Figure 4. - Variation of radiant heat flux with nozzle length. Reactor face temperature, 4680° R; wall temperature t_w, 1440° R; emissivity, 1.

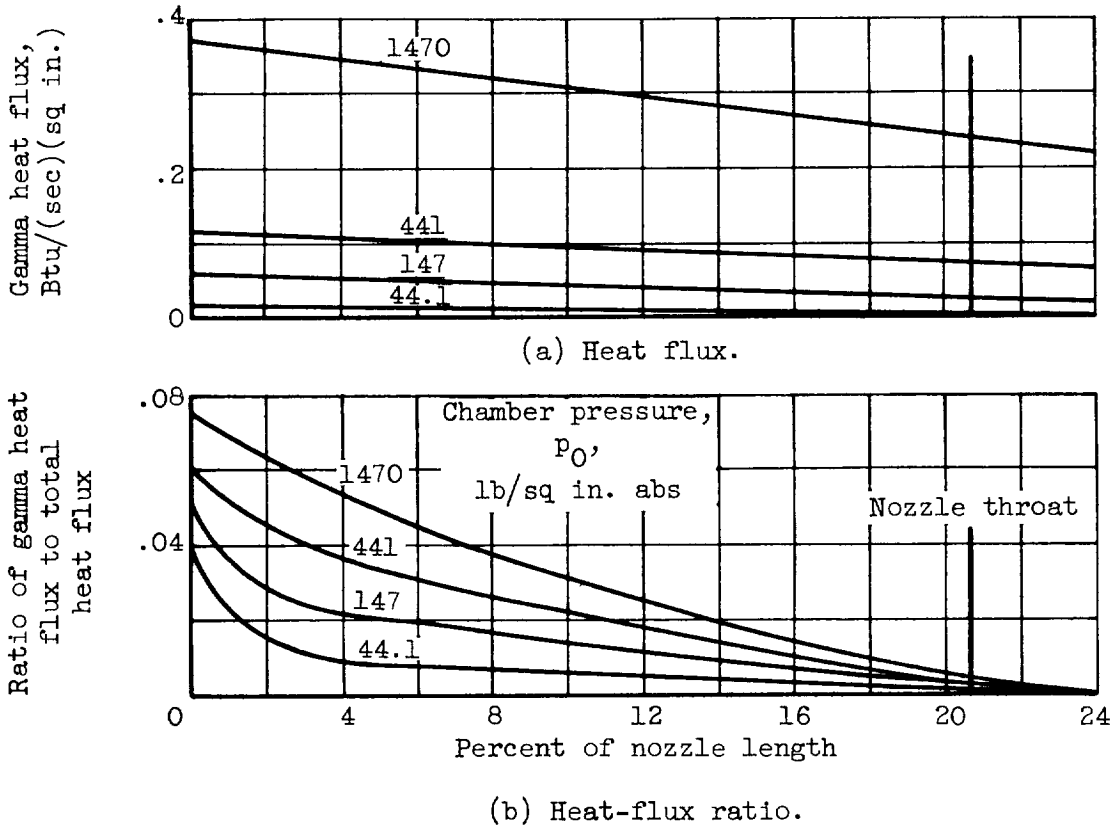

(a) Heat flux.

(b) Heat-flux ratio.

Figure 5. - Variation of gamma heat flux with nozzle length. Material, nickel; wall thickness, 0.020 inch.

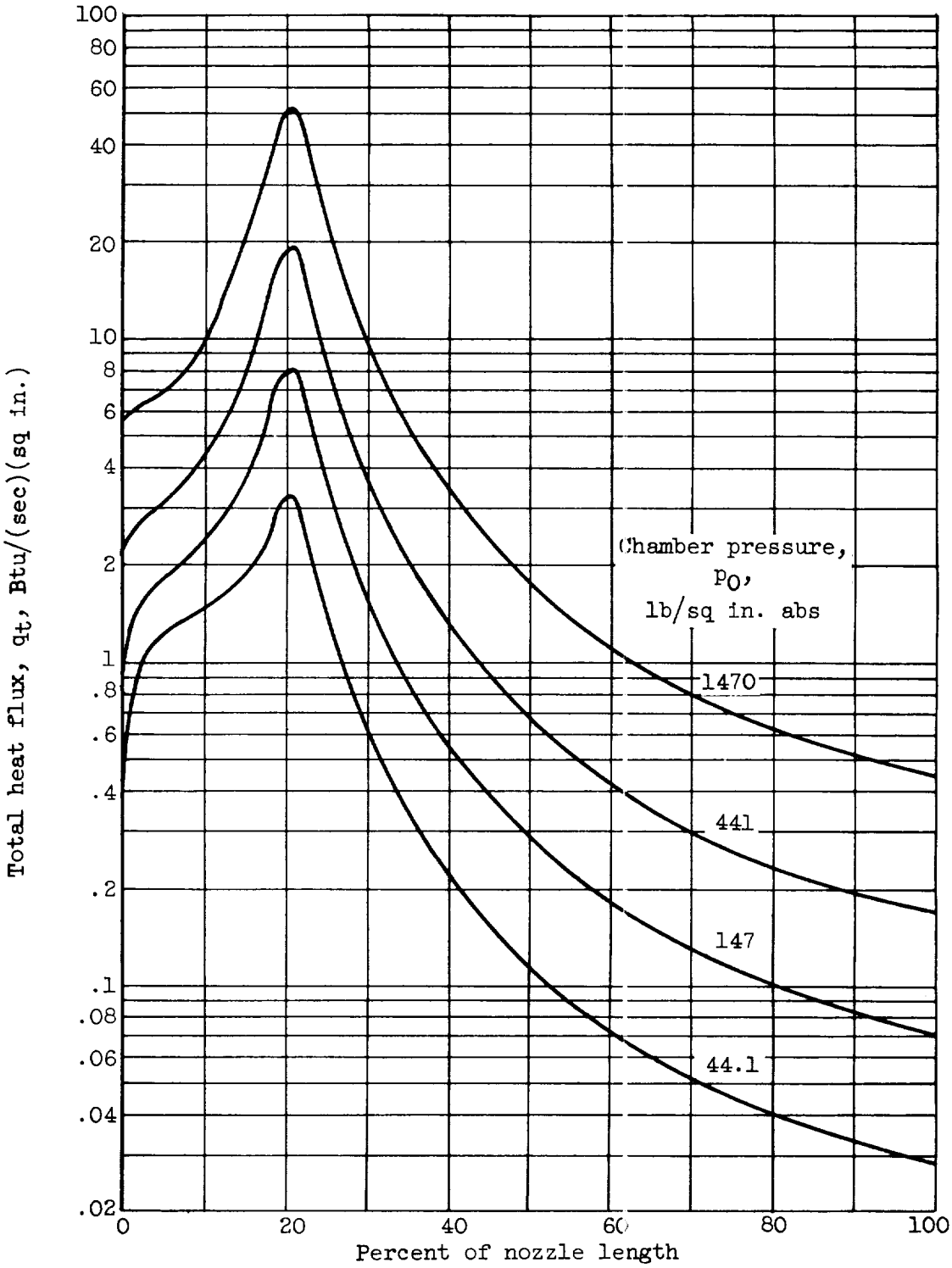

Figure 6. - Variation of total heat flux with nozzle length for various chamber pressures. Chamber temperature t_o, 4680° R; wall temperature t_w, 1440° R.

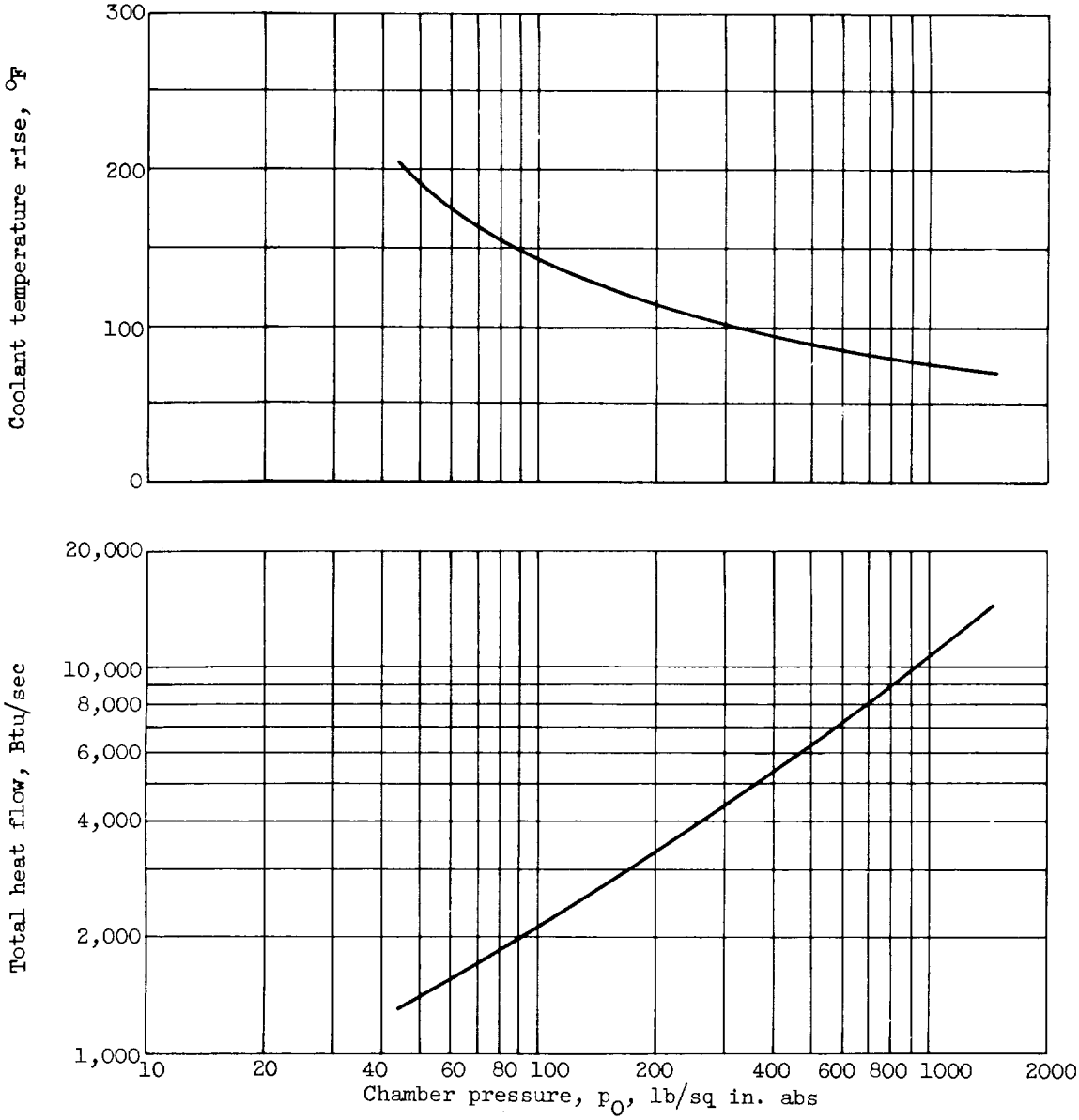

Figure 7. - Variation of heat flow and coolant temperature rise with chamber pressure. Chamber temperature t_o, 4680° R; wall temperature t_w, 1440° R.

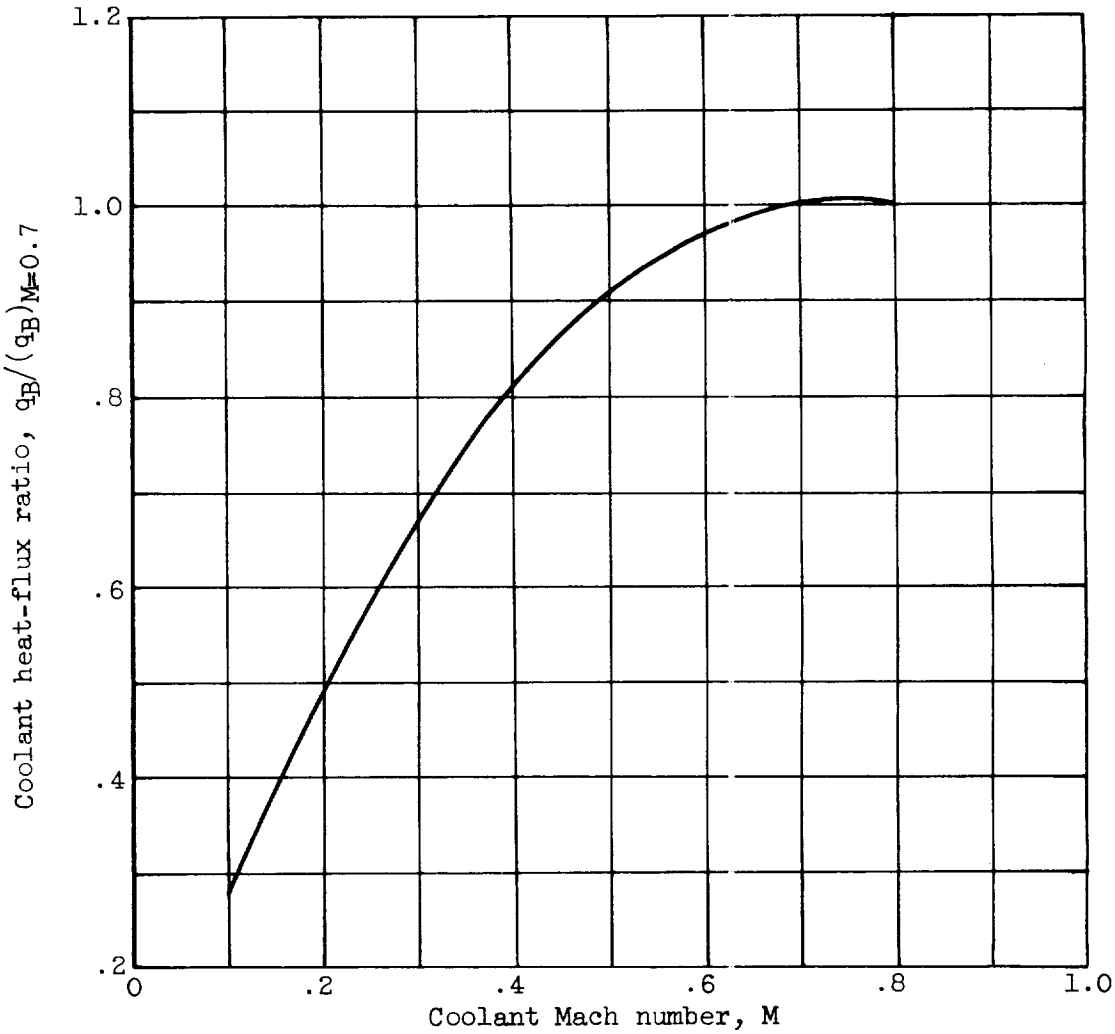

Figure 8. - Typical variation of coclant heat-flux ratio with Mach number.

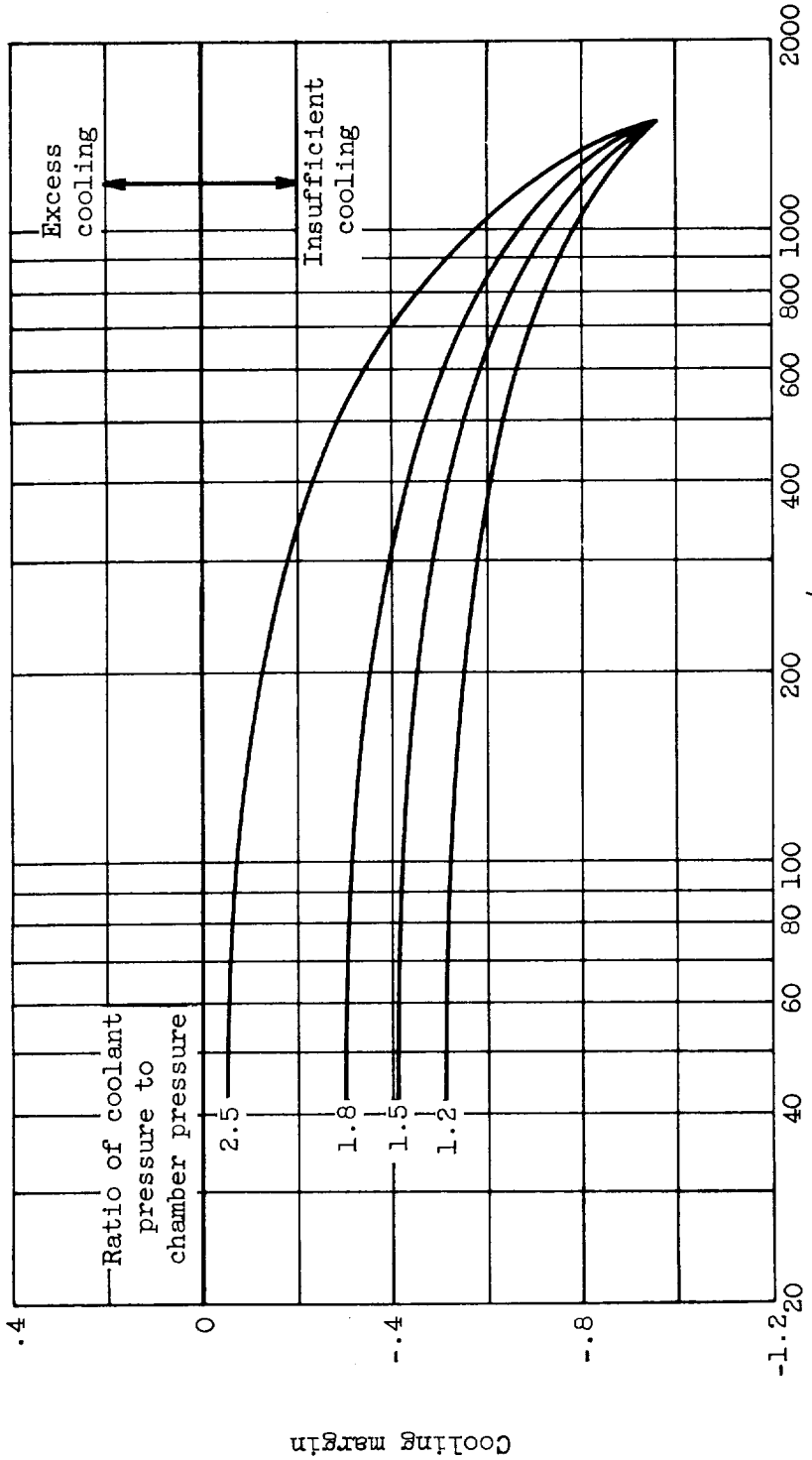

Figure 9. - Variation of cooling margin at throat with chamber pressure and system pressure ratio. Chamber temperature t_o, 4680° R; wall temperature t_w, 1440° R; coolant Mach number, 0.7.

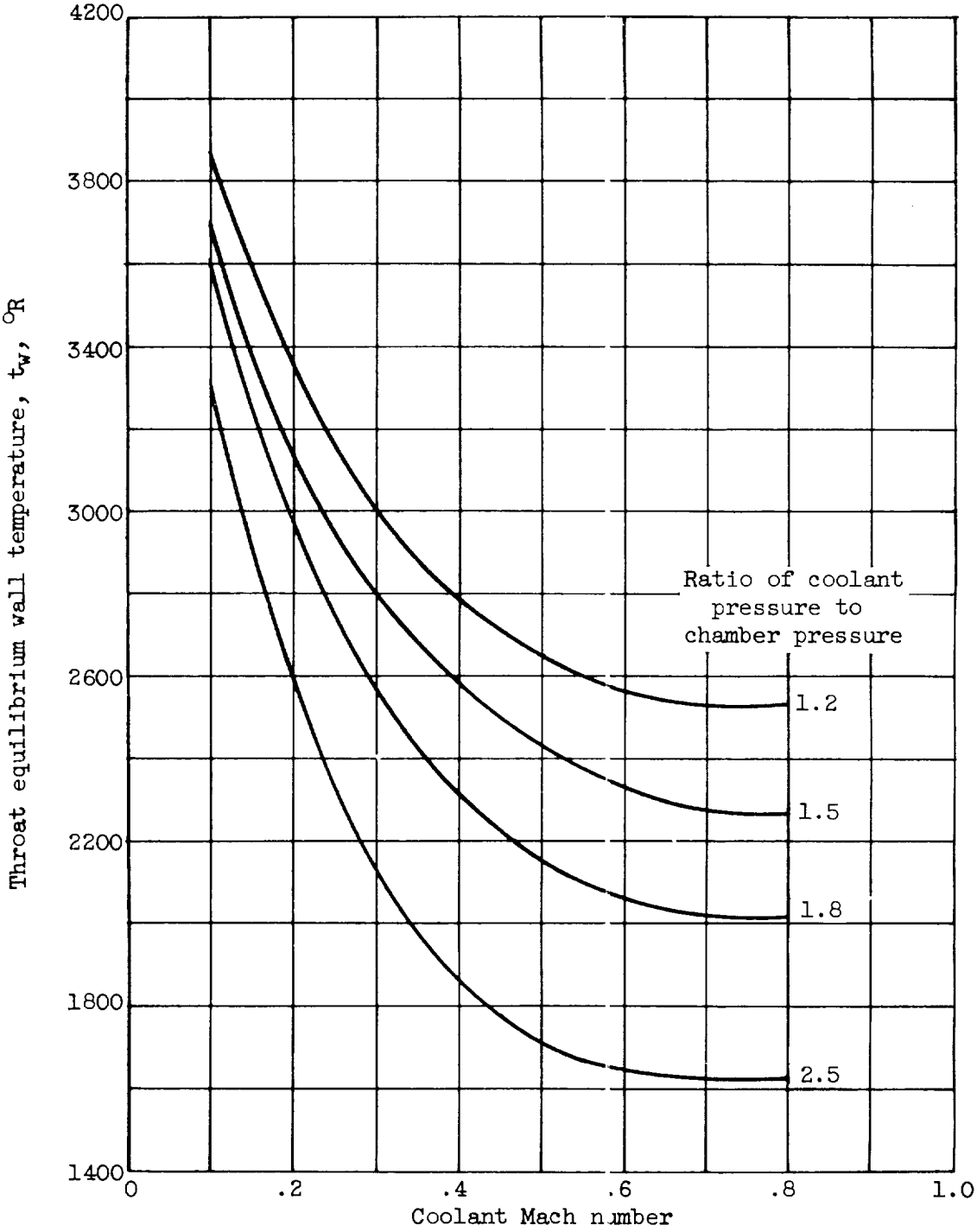

Figure 10. - Variation of throat equilibrium wall temperature with coolant Mach number and system pressure ratio. Chamber pressure p_o, 441 pounds per square inch absolute; chamber temperature t_o, 4680° R.